



Published in final edited form as:

*Strabismus*. 2018 March ; 26(1): 33–41. doi:10.1080/09273972.2017.1418393.

## Knobby Eye Syndrome

Joseph L. Demer, MD, PHD

Stein Eye Institute and Department of Neurology, Neuroscience Interdepartmental Program, and Bioengineering Interdepartmental Program, University of California, Los Angeles, USA

### Abstract

**Introduction**—A spherical globe is traditionally assumed, but this study employed magnetic resonance imaging (MRI) to demonstrate frequent occurrence of non-spherical staphylomata in strabismic patients.

**Methods**—High-resolution, surface coil MRI was obtained in multiple image planes in 21 highly myopic subjects (36 eyes) and compared with 17 normal controls (33 eyes). Images were analyzed for axial length, aspect ratio of eye shape, and deflection of muscle paths.

**Results**—All but two high myopes had strabismus. While myopic globes were generally spherical in 10 myopic eyes including both orthotropic subjects, 15 globes exhibited diffuse posterior staphylomata, 16 equatorial staphylomata, and 4 both posterior and equatorial staphylomata. Equatorial scleral ectasias were positioned to contact and elongate paths of horizontal rectus muscles in some gaze positions. Axial length in myopes averaged  $28.8 \pm 3.8$  (SD) mm and did not differ significantly between regular vs. irregular staphylomata. Globe aspect ratios in the coronal, axial, and sagittal planes were significantly greater than normal in myopes ( $P < 0.005$ ), but correlated significantly with axial length only in the axial and sagittal planes ( $P < 0.03$ ). While myopes with irregular staphylomata were older at  $57 \pm 11$  years than subjects with spherical globes at  $24 \pm 8$  years ( $P < 0.0005$ ), other clinical features were similar.

**Conclusion**—Irregular equatorial or posterior staphylomata are common in strabismic axial high myopes, acting, like “cams” affixed to the normally spherical globe so that they may have no mechanical effect until rotating eccentrically against muscles. After rotational contact, staphylomata would nonlinearly increase muscle tension with further duction. Imaging may be clinically informative about this “knobby eye syndrome.”

### Keywords

Magnetic resonance imaging; myopia; staphyloma; strabismus

---

**CONTACT** Joseph L. Demer [jld@jsei.ucla.edu](mailto:jld@jsei.ucla.edu) Stein Eye Institute, UCLA, 100 Stein Plaza, Los Angeles, CA 90095-7002, USA. Color versions of one or more of the figures in the article can be found online at [www.tandfonline.com/istr](http://www.tandfonline.com/istr).

### Declaration of interest

The author reports no conflict of interest.

### FDA disclosure

MRI surface coils used in imaging are not FDA approved for this purpose.

## Introduction

Historical concepts of the anatomical basis of strabismus have generally assumed normal anatomy of the globe and extraocular muscles (EOMs), and then presumed or demonstrated abnormalities of EOM innervation, contractile force, or stiffness to account for abnormal rotational alignments of two spherical globes. Beginning in the late twentieth century, it was recognized that abnormalities of the connective tissue pulleys of the EOMs could misdirect EOM forces to misalign the globes.<sup>1-6</sup> Such pulley abnormalities are now believed to be congenital or acquired.<sup>7</sup>

A particularly striking form of acquired pulley heterotopy with limited abduction and supraduction occurs in highly myopic people, a condition known as *myopic strabismus fixus* or heavy eye syndrome (HES).<sup>8-11</sup> The globe is by definition elongated anteroposteriorly in axial myopia, with the elongation often nonuniform in the form of a posterior ectasia termed a staphyloma.<sup>12</sup> In HES, degeneration of the LR-LR ligament permits inferior shift of the lateral rectus (LR) pulley over the enlarged, myopic globe so that the abducting LR force is converted to infraducting force, with nasal displacement of the superior rectus (SR) relative to the globe.<sup>8,10,11</sup> The HES may be viewed as a superotemporal luxation of the entire globe relative to the array of rectus muscles. Notwithstanding the recognition of frequent occurrence of staphylomatous ectasia occurs in some 90% of highly myopic globes and is progressive with age,<sup>12,13</sup> studies of HES have generally not commented on a possible contribution of globe asphericity in highly myopic strabismus. One notable exception is an early report of Demer and von Noorden, who employed x-ray computed tomography and attributed restricted ocular rotation in a single strabismic patient to contact between a staphylomatous globe and the orbital walls.<sup>14</sup> Another early report of Ohta *et al.* suggested additional occurrence of globe elongation and contact with the orbital wall in HES.<sup>15</sup> Equatorial staphylomata have been recognized during retinal detachment surgery under the paths of rectus EOMs.<sup>16</sup> These early and scattered reports suggest that possible contribution of the staphylomatous globe to strabismus be reconsidered in the setting of axial myopia.

The present study employed high-resolution magnetic resonance imaging (MRI) to demonstrate evaluate globe shape in axial high myopia and to identify and characterize those with prominent equatorial staphylomata that deflect EOM paths and presumably alter motility patterns in strabismus.

## Subjects and methods

Subjects in this study were 21 consecutive highly myopic patients who participated in a prospective MRI study of strabismus at the University of California, Los Angeles, from 1991 to 2016. Patients were selected from a total of 689 strabismic, 6 amblyopic non-strabismic, and 140 normal control subjects and who underwent ophthalmological examination and surface coil MRI of the orbits after giving informed consent according to a protocol approved by the Institutional Review Board of the University of University of California, Los Angeles, and in conformity with the Health Information Portability and Accountability Act and the Declaration of Helsinki. Patients underwent visual acuity assessment, motility examination, slit lamp and fundoscopic examination, refraction, and

photography of ocular versions. However, since many patients and control subjects had previously undergone cataract or refractive surgery, and since axial length was directly measured, refractive error was not considered directly as a datum. High-resolution T1- or T2-weighted MRI was performed using a 1.5 T scanner (Signa; General Electric, Milwaukee, WI, USA) using technique previously described.<sup>17</sup> Imaging was performed while one eye was centrally fixating a fiber optic target, usually the eye being imaged, but sometimes with the fellow eye fixation due to the presence of extreme angle strabismus that precluded fixation by the imaged eye.

A control group was selected as all of the normal, non-strabismic subjects recruited by advertising who had undergone similar MRI during the same interval as the highly myopic cases. These subjects all underwent ophthalmic examination by the author in similar fashion to the myopic patients, but were required to have visual acuity of 20/20 or better in each eye with or without correction and normal ocular motility, as well as no history of prior ophthalmic surgery that cataract surgery was allowable in older subjects. There were no exclusions of control subjects for refractive error.

Images were digitally imported into the program *ImageJ64* (Rasband, W.S. ImageJ, U.S. National Institutes of Health, Bethesda, Maryland, [imagej.nih.gov/ij/](http://imagej.nih.gov/ij/)) for analysis. Axial globe length (AL) was measured using axial MRI.<sup>18</sup> Globe shape was initially evaluated qualitatively by inspection in axial, quasi-coronal (perpendicular to the long axis of the orbit), and quasi-sagittal (parallel to the long axis of the orbit) planes. It should be noted that, because the long axis of each orbit is oriented approximately 23° to the mid-sagittal plane, craniotopic coronal and sagittal planes differ by roughly this amount from the quasi-sagittal planes employed here that optimize imaging of the EOMs. In the image plane containing its largest cross section, the globe cross section including the cornea was digitally outlined in each of these planes, with each resulting contour automatically fit with an ellipse using the standard function in *ImageJ64*. Since the radius of curvature of the cornea is less than that of the sclera, this procedure results in greater asphericity of even an otherwise spherical sclera in the axial and quasi-sagittal planes than in the quasi-coronal plane.

Aspect ratio was used as a quantitative index of asphericity in each of the three image orthogonal planes (axial, coronal, sagittal) incorporating globe diameter and was computed as the ratio of major (longer) to minor (shorter) axes of the ellipse best fit to the globe cross section (Figure 1). Aspect ratio with unity value indicates a perfect circle, while aspect ratio progressively exceeding 1.0 indicates an increasingly elongated shape. Inclusion of the corneal contour resulted in aspect ratios exceeding 1.0 in the axial and sagittal planes even when the posterior sclera was spherical.

In some cases where subjects underwent strabismus surgery, staphylomata were recognized and photographed intraoperatively.

## Results

Identified for evaluation were MRI studies in a total of 21 highly myopic subjects, of whom 14 were women. Interpretable imaging was obtained in 36 eyes that were highly myopic.

Ten of the myopic globes were generally spherical in six subjects. Figure 1 illustrates such a spherical normal right eye without axial myopia, but the unilaterally axially myopic, esotropic left eye of the same anisometric subject exhibits diffuse posterior staphyloma giving the axial contour an elliptical shape.

Ten eyes of 7 myopic subjects had generally spherical shapes similar to the right eye in Figure 1, while one or both globes of the other 14 subjects exhibited prominent diffuse posterior (11 eyes, similar to Figure 1 left eye), equatorial (12 eyes), or combined posterior and equatorial staphylomata (4 eyes). Figure 2 is an example of a bilateral equatorial staphyloma located superotemporally in highly myopic subject 1. In this case, the focal ectasias are cam-like angulations along the path of the LR muscles bilaterally and were visible during strabismus surgery as bluish scleral elevations (Figure 3). These scleral ectasias were positioned to contact and elongate the paths of the horizontal rectus muscles in some gaze positions.

Figure 4 illustrates both equatorial and posterior staphylomata, with the former located superiorly between the LR and SR insertions on the sclera. Such staphylomata displace LR paths inferiorly. In addition, the right eye of subject in Figure 4 also has posterior staphylomata nasal and temporal to the optic nerve that were observed in these gaze positions to contact the MR and LR during both abduction and adduction, respectively (not shown), and a posterior staphyloma of the left eye observed to contact the LR during adduction (also not shown).

Posterior staphylomata in other subjects were more angulated and associated with less prominent equatorial staphylomata as illustrated in Figure 5. These staphylomata also contacted the MR and LR during horizontal duction. Extremely irregular posterior scleral ectasias sometimes were associated with large displacements of EOM paths, as illustrated in Figure 6, where the LR path appears to be bilaterally shifted inferiorly. With the foregoing exemplars in mind, quantitative MRI analyses are presented below.

Subject ages and ALs are summarized in Table 1. Pooling all myopic eyes, AL averaged  $28.8 \pm 3.8$  mm, highly significantly greater than the corresponding control value of  $24.1 \pm 0.8$  mm ( $P < 10^{-7}$ ). However, AL was related to staphyloma shape, averaging (SD)  $26.3 \pm 0.7$  mm for myopic eyes without staphylomata and  $27.8 \pm 2.4$  mm for myopic eyes with equatorial staphylomata ( $P > 0.05$ ), but significantly more than both of the former at  $31.3 \pm 3.7$  mm in myopic eyes with diffuse posterior staphylomata ( $P < 0.005$ ). Ages of subjects with diffuse ( $54.1 \pm 12.8$  years) or equatorial ( $64.6 \pm 13.1$  years) staphylomata were significantly greater than normal controls or myopes with normal globe shape ( $P < 0.003$ ) that in turn did not differ significantly from one another ( $P > 0.4$ ). Since many of the subjects had undergone cataract or refractive surgery, no clinical features distinguished myopic subjects with diffuse from equatorial staphylomata.

Aspect ratio in axial myopes was significantly greater than control in all three image planes ( $P < 0.01$  after correction for multiple comparisons). While there was no correlation between aspect ratio and AL in controls in any of the three imaging orientations, linear regression

demonstrated that aspect ratio was significantly positively correlated with AL in the high myopes in the sagittal and axial, but not coronal, image planes ( $P < 0.05$ , Figure 7).

## Discussion

Contrary to historical assumptions of globe sphericity made by both clinical strabismologists and basic scientists, irregular equatorial or posterior staphylomata were commonly encountered here in strabismic axial high myopes, confirming ultrasonographic findings of staphylomatous changes correlated with myopic retinal degeneration in myopes generally,<sup>13</sup> as well as MRI findings in non-strabismic myopes.<sup>19</sup> Prior to MRI, these staphylomata were often unsuspected by both the patients and their strabismologists, so in the absence of preoperative imaging the staphylomata would either have remained occult or surprised operating strabismus surgeons with the finding of thin, dark sclera illustrated in Figure 3. These knobby staphylomata probably influence ocular motility. Staphylomata such as illustrated in Figures 4–6 may have configurations causing them to act like “cams” affixed to the normally spherical globe; thus, staphylomata could have no mechanical effect until they eccentrically rotate against EOM. After rotational contact, staphylomata would add tension to the EOM that increases nonlinearly with further duction. It is proposed that the mechanical effects of irregular staphylomata on EOM function be termed the “knobby eye syndrome,” nomenclature paralleling the existing terms for strabismus that can occur in high myopia: “heavy eye syndrome” describing inferonasal positioning of the LR and nasal position of the SR paths, both closely apposed to the superotemporally displaced globe<sup>9</sup>; and “sagging eye syndrome describing age-related inferolateral shift of the LR path<sup>20</sup> that also occurs in the absence of myopia.<sup>21</sup>

Strabismus surgeons are likely to encounter patients with high axial myopia since the prevalence of strabismus approaches 15% in this group<sup>22</sup> and since axial myopia now has extremely high prevalence worldwide, especially in East Asians.<sup>23–25</sup> The present study supports claims that staphylomata in high myopes are increasingly common with age<sup>13,25</sup> since irregular staphylomata were significantly more common in older than younger patients. Because axial and sagittal aspect ratio correlated significantly with axial length (Figure 7), strabismus surgeons should be increasingly suspicious of the presence of the knobby eye phenomenon in the presence of greater degrees of axial myopia. However, prominent staphylomata of this kind have been described in elderly Asian patients with degenerative myopia but axial lengths shorter than 26.5 mm.<sup>19</sup> Of course, in patients who are pseudophakic or who were previously undergoing refractive surgery, current refractive state does not reflect the increased AL associated with the original myopia. Characteristic ophthalmoscopic changes can provide clues to the existence of axial myopia that can be readily verified by ultrasound, computed x-ray tomography, or MRI.<sup>13</sup> Posterior staphylomata may also be detectable by widefield optical coherence tomography,<sup>26</sup> although this imaging technique would not be sensitive to diffuse posterior staphylomata larger than the field of imaging or any anterior staphylomata outside the field of imaging.

The causes of the current worldwide epidemic of myopia are unknown, but one recent hypothesis involves EOM force. Even in normal people, optic nerve length (ON) is insufficient to permit full adduction without tethering of the globe by the taut ON.<sup>18,27</sup> This

tethering phenomenon exerts maximal traction on the temporal peripapillary sclera between the optic nerve head and fovea, the typical site of myopic peripapillary atrophy and posterior staphylomata,<sup>13,28–31</sup> and produces temporal optic disc tilting in adduction visible by optical coherence tomography.<sup>32,33</sup> Both axial high myopia and esotropia are associated with reduced ON length.<sup>18</sup>

Several limitations exist for this study. The patient base included a relatively small number of strabismic subjects with staphylomata and did not include a large number of orthotropic myopes. It is therefore impossible to quantify the prevalence of knobby eye syndrome among either strabismic or myopic patients generally. Axial lengths were measured in this study using MRI and may not precisely correspond to ultrasonographic measures. It was impossible to correlate findings with phakic refractions since many myopic subjects had previously undergoing cataract or refractive surgery that optically offset their prior myopia. Quantitative analysis of three-dimensional eye shape was not possible since complete, multiplanar imaging of each globe was generally not performed. Finally, there currently exists no adequate biomechanical model to generally compute the effects of irregular staphylomata; all existing models of binocular alignment, the most complete being *Orbit 1.8*, assume a spherical globe.<sup>34</sup>

Even when myopic patients do not exhibit the extreme findings of the HES,<sup>8,11,35–37</sup> the present study suggests that myopic changes may contribute to strabismus. Concepts of strabismus in axial high myopes should be expanded to include nonlinear changes in EOM tension produced by irregular posterior staphylomata; imaging may be clinically informative about the knobby eye syndrome. The possibility of knobby eye syndrome should be considered in the clinical evaluation of strabismic patients who are currently myopic, and especially in elderly pseudophakic patients who may have been myopic prior to cataract surgery, and who thus are more likely to have irregular staphylomata.

## Acknowledgments

### Funding

U.S. Public Health Service, National Institutes of Health, National Eye Institute grant EY008313, and an Unrestricted Grant from Research to Prevent Blindness.

## References

1. Clark RA, Miller JM, Rosenbaum AL, Demer JL. Heterotopic muscle pulleys or oblique muscle dysfunction? *J Aapos*. 1998; 2:17–25. [PubMed: 10532362]
2. Demer, JL., Clark, RA., Miller, JM. Heterotopy of extraocular muscle pulleys causes incomitant strabismus. In: Lennerstrand, G., editor. *Advances in Strabismology*. Buren, Netherlands: Aeolus Press; 1999. p. 91-94.
3. Oh SY, Clark RA, Velez F, Rosenbaum AL, Demer JL. Incomitant strabismus associated with instability of rectus pulleys. *Invest Ophthalmol Vis Sci*. 2002; 43:2169–2178. [PubMed: 12091413]
4. Piruzian A, Goldberg RA, Demer JL. Inferior rectus pulley hindrance: orbital imaging mechanism of restrictive hypertropia following lower lid surgery. *J Aapos*. 2004; 8:338–344. [PubMed: 15314594]
5. Kono R, Okanobu H, Ohtsuki H, Demer JL. Displacement of the rectus muscle pulleys simulating superior oblique palsy. *Jpn J Ophthalmol*. 2008; 52:36–43. [PubMed: 18369698]

6. Demer, JL., Kono, R., Wright, W., Oh, SY., Clark, RA. Gaze-related orbital pulley shift: a novel cause of incomitant strabismus. In: De Faber, JT., editor. Progress in Strabismology. Lisse: Swets and Zeitlinger; 2002. p. 207-210.
7. Demer JL. The Apt lecture. connective tissues reflect different mechanisms of strabismus over the life span. J APOS. 2014; 18(4):309–315.
8. Krzizok T, Wagner D, Kaufmann H. Elucidation of restrictive motility in high myopia by magnetic resonance imaging. Arch Ophthalmol. 1996; 115:1019–1027.
9. Yamaguchi M, Yokoyama T, Shiraki K. Surgical procedure for correcting globe dislocation in high-myopic strabismus. Am J Ophthalmol. 2010; 149(2):341–346. [PubMed: 19939345]
10. Krzizok TH, Schroeder BU. Measurement of recti eye muscle paths by magnetic resonance imaging in highly myopic and normal subjects. Invest Ophthalmol Vis Sci. 1999; 40(11):2554–2560. [PubMed: 10509649]
11. Krzizok TH, Kaufmann H, Traupe H. New approach in strabismus surgery in high myopia. Br J Ophthalmol. 1997; 81(8):625–630. [PubMed: 9349146]
12. Frisina R, Baldi A, Cesana BM, Semeraro F, Parolini B. Morphological and clinical characteristics of myopic posterior staphyloma in Caucasians. Graefes Arch Clin Exp Ophthalmol. 2016; 254(11):2119–2129. [PubMed: 27106626]
13. Hsiang HW, Ohno-Matsui K, Shimada N, et al. Clinical characteristics of posterior staphyloma in eyes with pathologic myopia. Am J Ophthalmol. 2008; 146(1):102–110. [PubMed: 18455142]
14. Demer JL, Von Noorden GK. High myopia as an unusual cause of restrictive motility disturbance. Surv Ophthalmol. 1989; 33:281–284. [PubMed: 2652362]
15. Ohta M, Iwashige H, Hayashi T, Maruo T. [Computed tomography findings in convergent strabismus fixus]. Nippon Ganka Gakkai Zasshi. 1995; 99(8):980–985. [PubMed: 7676901]
16. Robertson DM. Retinal detachment with equatorial staphyloma. Arch Ophthalmol. 1996; 114(4):496–497. [PubMed: 8602796]
17. Demer JL, Dusyanth A. T2 fast spin echo magnetic resonance imaging of extraocular muscles. J APOS. 2011; 15:17–23.
18. Demer JL. Optic nerve sheath as a novel mechanical load on the globe in ocular duction. Invest Ophthalmol Vis Sci. 2016; 57(4):1826–1838. [PubMed: 27082297]
19. Wang NK, Wu YM, Wang JP, et al. Clinical characteristics of posterior staphylomas in myopic eyes with axial length shorter than 26.5 millimeters. Am J Ophthalmol. 2016; 162:180–190 e181. [PubMed: 26585213]
20. Tan RJ, Demer JL. Heavy eye syndrome versus sagging eye syndrome in high myopia. J APOS. 2015; 19(6):500–506.
21. Rutar T, Demer JL. “Heavy eye syndrome” in the absence of high myopia: A connective tissue degeneration in elderly strabismic patients. J Aapos. 2009; 13:36–44. [PubMed: 18930668]
22. Tanaka A, Ohno-Matsui K, Shimada N, et al. Prevalence of strabismus in patients with pathologic myopia. J Med Dent Sci. 2010; 57(1):75–82. [PubMed: 20437768]
23. Nakao Y, Kimura T. Prevalence and anatomic mechanism of highly myopic strabismus among Japanese with severe myopia. Jpn J Ophthalmol. 2014; 58(2):218–224. [PubMed: 24390603]
24. Pan CW, Dirani M, Cheng CY, Wong TY, Saw SM. The age-specific prevalence of myopia in Asia: A meta-analysis. Optom Vis Sci. 2015; 92:258–266. [PubMed: 25611765]
25. Gupta P, Cheung CY, Saw SM, et al. Peripapillary choroidal thickness in young Asians with high myopia. Invest Ophthalmol Vis Sci. 2015; 56(3):1475–1481. [PubMed: 25655797]
26. Shinohara K, Shimada N, Moriyama M, et al. Posterior staphylomas in pathologic myopia imaged by widefield optical coherence tomography. Invest Ophthalmol Vis Sci. 2017; 58(9):3750–3758. [PubMed: 28738419]
27. Demer JL, Clark RA, Suh SY, et al. Magnetic resonance imaging of optic nerve traction during adduction in primary open-angle glaucoma with normal intraocular pressure. Invest Ophthalmol Vis Sci. 2017; 58(10):4114–4125. [PubMed: 28829843]
28. Akagi T, Hangai M, Kimura Y, et al. Peripapillary scleral deformation and retinal nerve fiber damage in high myopia assessed with swept-source optical coherence tomography. Am J Ophthalmol. 2013; 155(5):927–936. [PubMed: 23434206]

29. Nakazawa M, Kurotaki J, Ruike H. Longterm findings in peripapillary crescent formation in eyes with mild or moderate myopia. *Acta Ophthalmol.* 2008; 86(6):626–629. [PubMed: 18577184]
30. Samarawickrama C, Mitchell P, Tong L, et al. Myopia-related optic disc and retinal changes in adolescent children from Singapore. *Ophthalmology.* 2011; 118(10):2050–2057. [PubMed: 21820741]
31. Kim TW, Kim M, Weinreb RN, Woo SJ, Park KH, Hwang JM. Optic disc change with incipient myopia of childhood. *Ophthalmology.* 2012; 119(1):21–26. e21–23. [PubMed: 21978594]
32. Chang MY, Shin A, Park J, et al. Deformation of optic nerve head and peripapillary tissues by horizontal duction. *Am J Ophthalmol.* 2016; 174:85–94. [PubMed: 27751810]
33. Suh SY, Le A, Shin A, Park J, Demer JL. Progressive deformation of the optic nerve head and peripapillary structures by graded horizontal duction. *Invest Ophthalmol Vis Sci.* 2017; 58(12): 5015–5021. [PubMed: 28973373]
34. Miller, JM., Pavlovski, DS., Shaemeva, I. *Orbit 1.8 Gaze Mechanics Simulation.* San Francisco: Eidactics; 1999.
35. Rowe FJ, Noonan CP. Surgical treatment for progressive esotropia in the setting of high-axial myopia. *J Aapos.* 2006; 10:596–597. [PubMed: 17189163]
36. Aydin P, Kansu T, Sanac AS. High myopia causing bilateral abduction deficiency. *J Clin NeuroOphthalmol.* 1992; 12:163–165. [PubMed: 1401160]
37. Aoki Y, Nishida Y, Hayashi O, et al. Magnetic resonance imaging measurements of extraocular muscle path shift and posterior eyeball prolapse from the muscle cone in acquired esotropia with high myopia. *Am J Ophthalmol.* 2003; 136:482–489. [PubMed: 12967802]



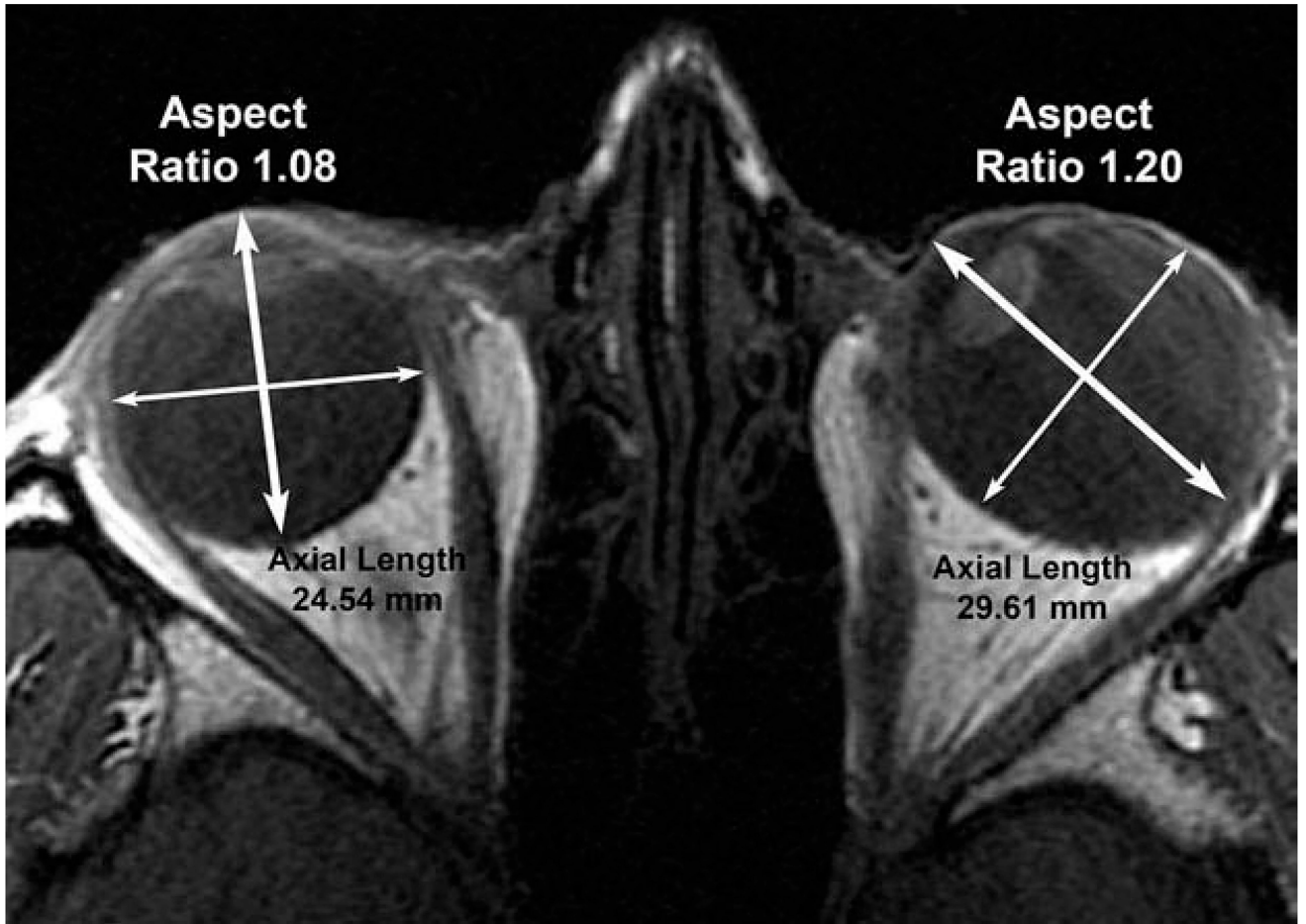


**Figure 1.**

Axial MRI of subject with unilateral axial myopia in esotropic left eye. Major axes of ellipses fitting each globe cross section are indicated by bold bidirectional arrows and minor axes by thin arrows. Emmetropic right eye cross section is nearly circular even including the cornea for aspect ratio 1.08, while cross section of diffusely staphylomatous, myopic left eye is oval with aspect ratio 1.20. Axial length of the myopic left eye is about 5 mm greater than the emmetropic right eye.

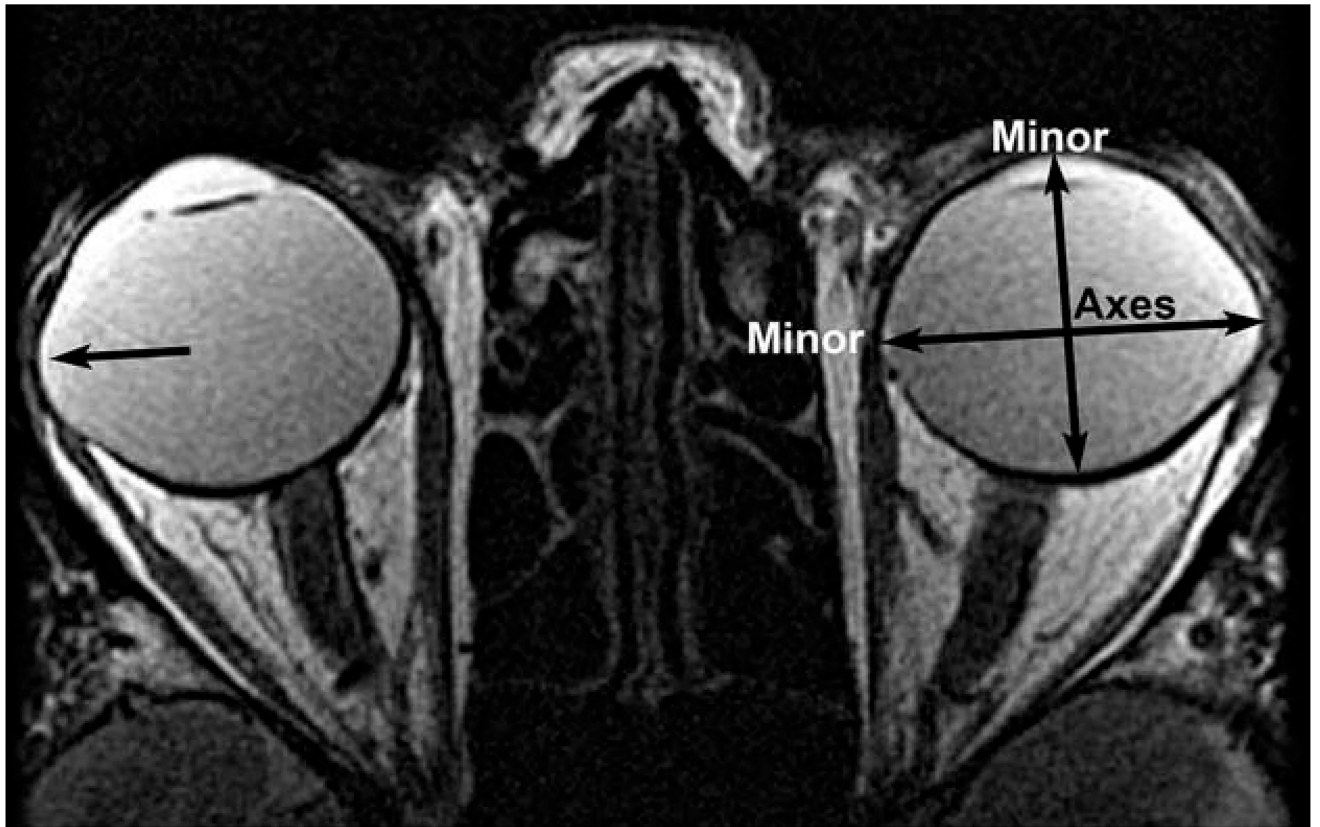


**Figure 2.** Axial MRI showing equatorial staphylomata (horizontal arrows) in high myopic subject 1. Vertical lines indicate minor axis of fitted ellipse. In this and subsequent figures, the right eye is shown on the left, and the left eye on right.

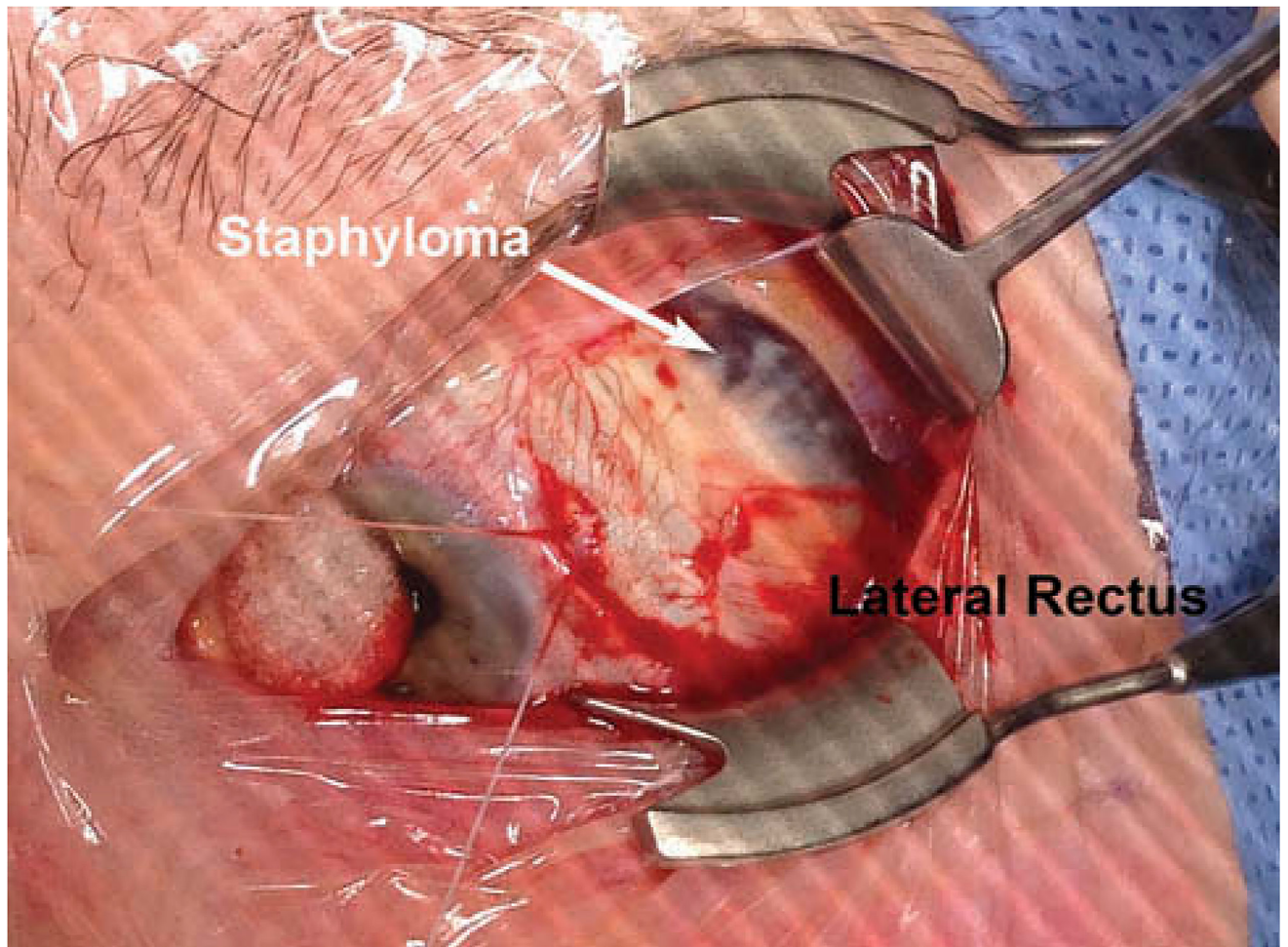


**Figure 3.** Intraoperative photo of superotemporally located equatorial staphylomata (dark sclera) in the left eye of myopic subject 1 whose MRI is presented in Figure 2.



**Figure 4.** Axial (upper row) and quasi-coronal (lower row) MRI showing equatorial and posterior staphylomata denoted by arrows in highly myopic subject 2.

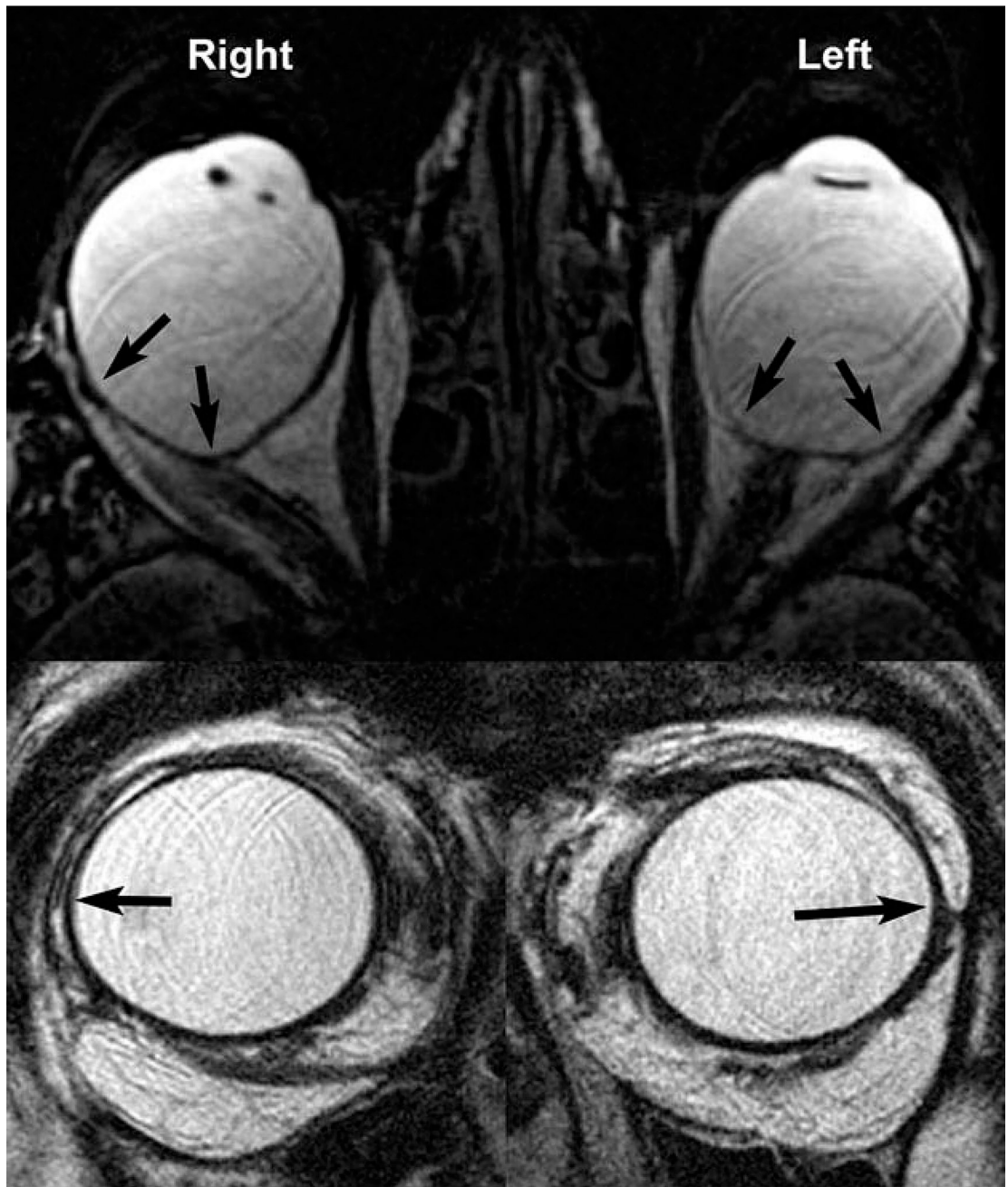


**Figure 5.** Axial (upper row) and quasi-coronal (lower row) MRI showing posterior and equatorial staphylomata denoted by arrows in subject 3.

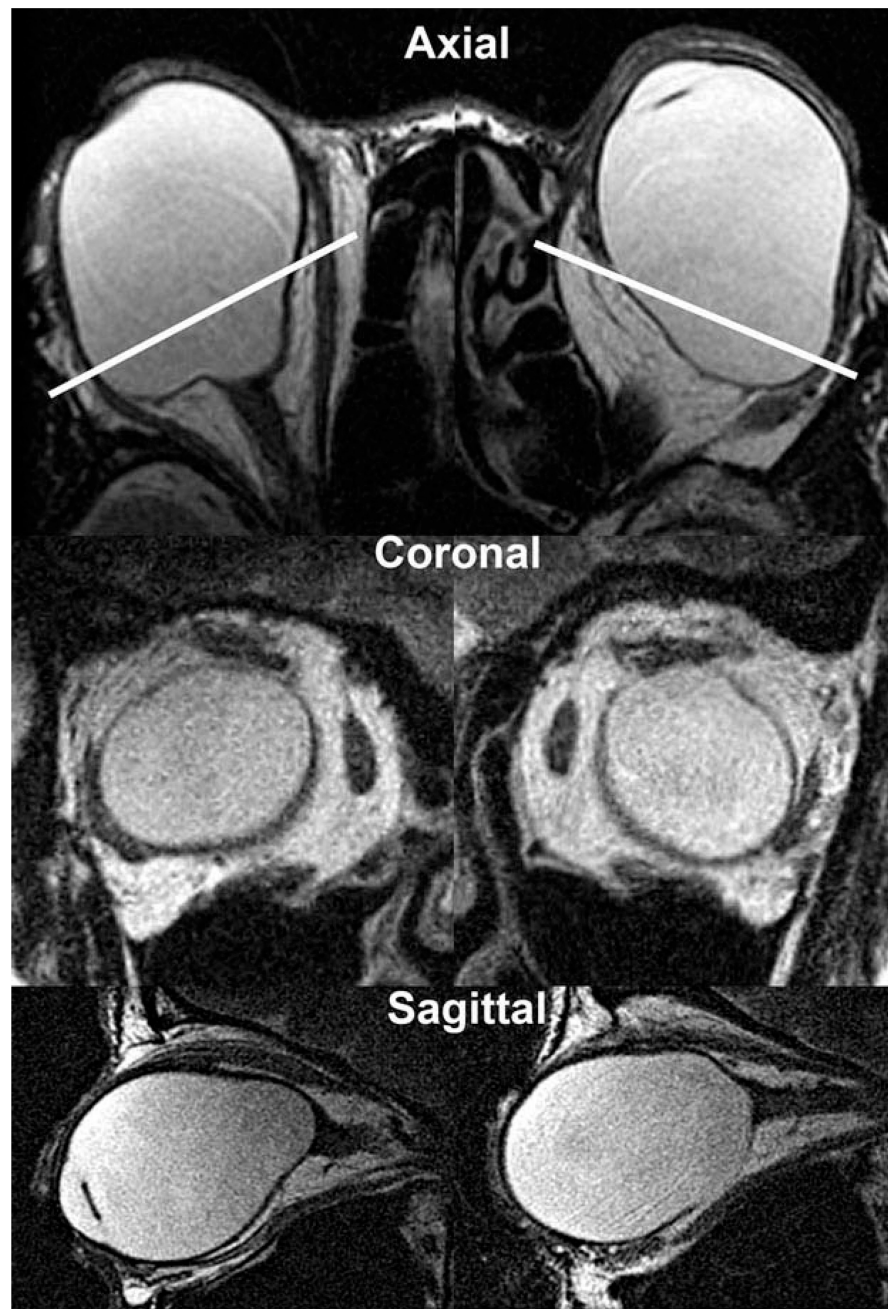


**Figure 6.** Axial (upper row) and quasi-coronal (middle row) and quasi-sagittal MRI in bilaterally pseudophakic high myopic subject 4 exhibiting prominent knobby posterior staphylomata. White lines in upper row indicate the imaging planes of the quasi-coronal images in the middle row.

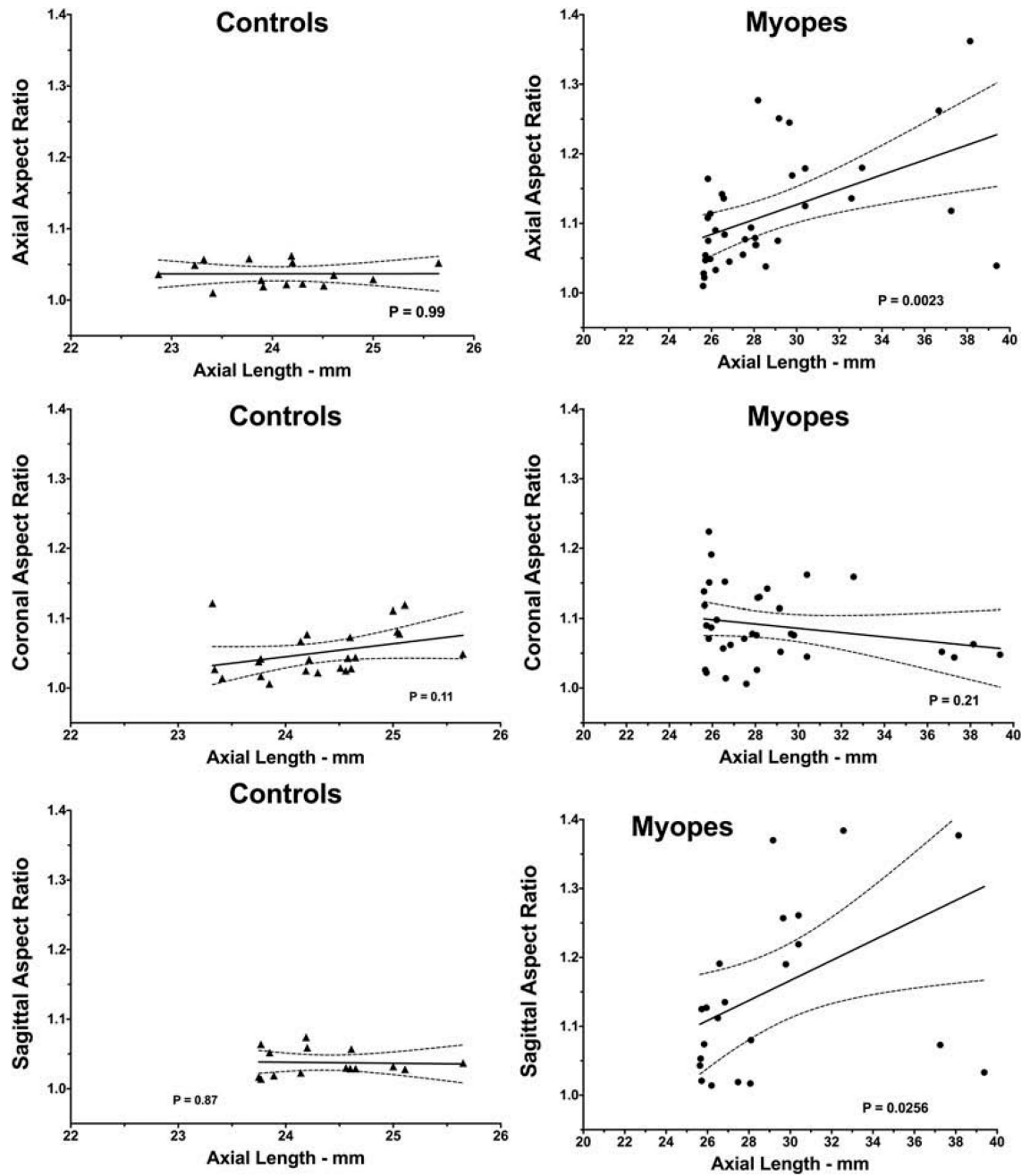


**Figure 7.** Correlations between axial globe length and aspect ratio in axial, coronal, and sagittal planes. Dotted lines indicate 95% confidence limits of linear regression fits.

**Table 1**

## Ages and Axial Lengths

Group	<u>Age, years</u>		<u>Axial Length, mm</u>	
	Mean	SD	Mean	SD
<b>Control</b>	28.0	15.7	24.1	0.8
<b>Myopic Normal Shape</b>	33.2	6.3	26.3	0.7
<b>Myopic Diffuse Staphyloma</b>	54.1	12.8	33.1	3.7
<b>Myopic Equatorial Staphyloma</b>	64.6	13.1	27.8	2.4

Author Manuscript

Author Manuscript

Author Manuscript

Author Manuscript